Materials Science and Engineering A 462 (2007) 259–263

MATERIALS SCIENCE & ENGINEERING A

www.elsevier.com/locate/msea

Dynamic softening of ferrite during large strain warm deformation of a plain-carbon steel

B. Eghbali [a,*], A. Abdollah-zadeh [b], P.D. Hodgson [c]

[a] *Department of Materials Engineering, Sahand University of Technology, P.O. Box 51335-1996, Tabriz, Iran*
[b] *Department of Materials Engineering, Tarbiat Modares University, P.O. Box 14115-143, Tehran, Iran*
[c] *School of Engineering, and Technology, Deakin University, Waurn Ponds, Geelong, Vic. 3217, Australia*

Received 31 August 2005; received in revised form 21 March 2006; accepted 11 April 2006

Abstract

The evolution of dynamic ferrite softening in a plain-carbon steel was investigated by torsion tests during warm deformation at 810 °C, in the two-phase (ferrite + austenite) region, and strain rate of 0.1 s^{-1} with different strains up to 50. The warm flow behaviour and ferrite microstructural parameters, such as grain size, misorientation angle across ferrite/ferrite boundaries, and the fraction of high-angle and low-angle grain/subgrain boundaries were quantified using electron back scatter diffraction. The results show that with increasing strain up to ∼2, the ferrite grain size and fraction of high-angle boundaries rapidly decrease and the fraction of low-angle boundaries increases. However, these parameters remain approximately unchanged with increasing strain from ∼2 to 50. The dynamic softening mechanism observed during large strain ferritic deformation is explained by dynamic recovery and continuous dynamic recrystallization.

Keywords: Warm deformation; Ferrite; Dynamic softening; Continuous dynamic recrystallization; C-Mn steel

1. Introduction

Warm, or ferritic, deformation has long been a topic of investigations by metallurgists as it is one of the key factors responsible for the properties of final products. Recently, this process has received considerable interest due to its potential to broaden the product range and reduce the production costs [1–5].

However, the control of the strip thickness and the final properties are much more complex than in the standard austenite rolling processes. The origin of the increased complexity is from the number of possible events that can occur during deformation: austenite softening, ferrite softening, and strain-induced transformation. Extensive research has been undertaken on some of these processes; in particular the recrystallization of austenite [6–8] and strain-induced transformation [9–12], but so far ferrite softening, in particular dynamic softening in the ferrite state, has received limited attention [13]. In most cases, it has been found that dynamic recovery (DRC) is the sole dynamic softening mechanism in ferrite due to its high stacking-fault energy (SFE) [14,15]. Discontinuous dynamic recrystallization is found to occur only in high purity ferrite and in ferritic interstitial-free steels [16]. It has been reported [17–19] that the other type of dynamic softening is continuous dynamic recrystallization (CDRX) that occurs in high SFE metals. The CDRX is the phenomenon in which misorientation across low-angle boundaries increases continuously with increasing strain until the low-angle boundaries change to high-angle grain boundaries so that grains are subdivided [18,20,21]. Because it leads to significant grain refinement during hot deformation [22,23], CDRX is likely to have potential industrial interest regarding the thermomechanical processing of high SFE alloys. A better knowledge and control of this mechanism should contribute to improvement of the deformation schedules of such materials. Only limited data are available in the literature for the dynamic flow softening during the large strain warm deformation of C-Mn steels.The aim of the present research is to study the mechanisms of extended dynamic flow softening of ferrite during warm torsion testing of a C-Mn steel, with particular attention to the effect of large strain on the ferrite microstructure characterized by the electron back scatter diffraction (EBSD) technique.

* Corresponding author. Tel.: +98 412 3443801x2118; fax: +98 412 3444333.
E-mail address: eghbali@sut.ac.ir (B. Eghbali).

0921-5093/$ – see front matter © 2006 Elsevier B.V. All rights reserved.
doi:10.1016/j.msea.2006.04.154

2. Material and experimental procedure

2.1. Material

A commercial low carbon steel was used in this study. The chemical composition (mass%) was 0.055C, 0.006Si, 0.21Mn, 0.011P, 0.013S, 0.037Al, and balance Fe. Torsion samples with a gauge of 20 mm length and 6.7 mm diameter were machined from the as-received plates with the longitudinal axis parallel to the rolling direction.

2.2. Torsion test procedure

Warm deformation tests were performed on a torsion rig described elsewhere [24]. Initially a continuous cooling torsion test was used to measure the critical transformation temperatures. The Ar_1 and Ar_3 temperatures were found to be 800 and 856 °C, respectively.

The deformation schedule for the study of the microstructure evolution involved austenitization at 1000 °C for 2 min, followed by cooling at a rate of 1 K/s to a deformation temperature of 876 °C (in the austenite region) and a hold of 120 s to homogenize the temperature within the samples. At this temperature, a single roughing pass was conducted with a strain of 2 and a strain rate of 1 s^{-1}. The samples were then cooled to a warm deformation temperature of 810 °C, in the two-phase ($\alpha + \gamma$) region, and held for 120 s to equalize the temperature throughout the specimens that produced about 97% ferrite and 3% austenite. Then a single pass large strain ferrite deformation, up to 50, was conducted at a strain rate of 0.1 s^{-1}. At this ferrite deformation condition, the temperature profile did not rise through of large deformation within the two-phase region. The measured values of torque (T) and twist (θ) were converted to Von Mises effective stress and strain at the specimen surface using an in-house procedure by a computer program based on the following formulas [24]:

$$\sigma = \frac{3.3\sqrt{3}T}{2\pi R}, \qquad \varepsilon = \frac{\theta R}{\sqrt{3}L}$$

where L and R are the gauge length and its radius, respectively. To follow the evolution of the ferrite microstructure, the tests were interrupted at selected strains and the microstructure was retained by quenching the samples with water jet sprays immediately, 0.2 s, after deformation.

2.3. Microstructures characterization

Deformed samples with different strains were mounted so that the microstructure of the plane containing the shear direction and the shear plane normal could be examined. Specimens were prepared for EBSD analysis in the standard manner. EBSD was performed on a field-emission-gun Scanning Electron Microscope (SEM, LEO) equipped with HKL Channel 5 system software (HKL Technology, Hobro, Denmark). The SEM was operated at an accelerating voltage of 20 kV and area mapping for 210 μm × 150 μm was performed with a step size of 0.3 μm on a square grid so that the total step number was 350,000. In the data presented, high-angle boundaries (HABs) are defined as having misorientations greater than 15° and low-angle boundaries (LABs) are defined as having misorientations of 3–15°. Therefore, a minimum misorientation cut-off of 3° has been used to eliminate excessive misorientation noise [25,26].

3. Results

3.1. Warm flow curves

Fig. 1 presents the warm flow curves obtained from the torsion samples tested at first at 876 °C, in the γ region, as a roughing pass, and then at 810 °C, in the two-phase ($\alpha + \gamma$) region to strains up to 50. As can be seen in this figure, the ferrite flow curve increases and reaches its maximum at early stage of torsion testing then drops to a stable, steady-state stress. All of the second curves for different strains displayed a steady-state region with a distinct peak in the flow stress which is observed at large strain warm deformation. The degree of ferrite dynamic softening is relatively minor compared to the dynamic recrystallization of austenite during the roughing pass deformation at 876 °C. In addition, it is of interest to note that a completely extended steady state is observed through to very large strains of 50.

3.2. Ferrite grain size

The variation of ferrite grain size (defined as the average distance between HABs) with strain, measured by linear intercept method, is shown in Fig. 2. As can be seen, the grain size at the beginning of the deformation ($\varepsilon = 0$) is ~25 μm. During the early stages of deformation, as strain increases up to ~2, the average grain size considerably decreased to ~12 μm. With increasing strain the ferrite grain size does not change significantly.

3.3. Magnitudes of LABs and HABs

It is interesting to characterize the magnitude the of high-angle and low-angle boundaries expected to form with increas-

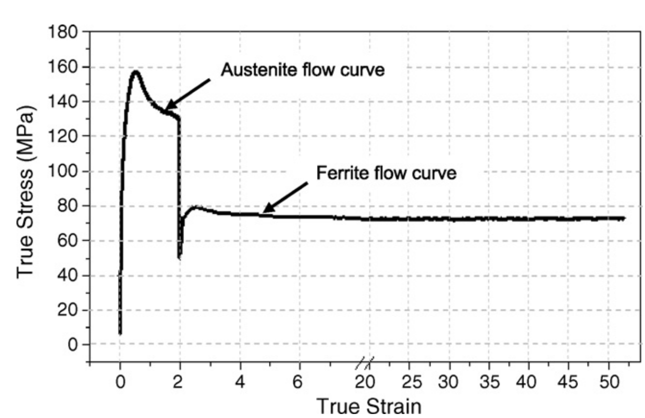

Fig. 1. The true stress–true strain flow curve of austenite and large strain warm deformed ferrite at 876 °C with strain rate of 1 s^{-1} and at 810 °C with strain rate of 0.1 s^{-1}, respectively.